

# Magnetohydrodynamic Simulation on Magnetic Compression Process of a Field-Reversed Configuration Plasma

KANKI Takashi, SUZUKI Yukihisa, OKADA Shigefumi and GOTO Seiichi  
Plasma Physics Laboratory, Graduate School of Engineering, Osaka University  
2-1 Yamada-oka, Suita, Osaka 565-0871, Japan

(Received: 8 December 1998 / Accepted: 19 February 1999)

## Abstract

A magnetic compression process of a field-reversed configuration (FRC) plasma is studied by means of a magnetohydrodynamic simulation. The simulations have been performed in the parameter range of the recent FRC Injection Experiment machine. It is shown from the simulation results that an axial magnetic compression enables an equilibrium transition from long and thin FRC to short and fat FRC. The effects of magnetic compression on the FRC plasmas are discussed.

## Keywords:

field-reversed configuration, magnetic compression, magnetohydrodynamic simulation

## 1. Introduction

A novel magnetic compression method of a field-reversed configuration (FRC) plasma has been proposed [1]. This method is an axial magnetic compression and has a possibility of equilibrium control and confinement improvement of an FRC plasma. The axial magnetic compression of an FRC plasma is accomplished by shortening the distance between a pair of the magnetic mirror fields at a confinement region. This compression results in the increase in the separatrix radius  $r_s$  and the decrease in the separatrix length  $l_s$ . In general, the large plasma radius will improve the magnetic decay and particle loss times. This confinement improvement can be explained by the empirical scaling law,  $\tau_N \propto R^2 / \rho_i$  [2]. Here  $\tau_N$ ,  $R$  and  $\rho_i$  represent the particle confinement time, the FRC major radius and the ion gyroradius in the external magnetic field, respectively.

On the FRC Injection Experiment (FIX) machine [3] at Osaka, the axial compressing magnetic field is applied to a translated FRC plasma which eventually settles down in the confinement region [4]. However, details concerning how such a compression process of

an FRC plasma is performed by the compressing magnetic field remain unclear.

Under this experimental background, the purpose of this study is to investigate the fundamental physics of magnetic compression process of an FRC plasma by means of an axisymmetric numerical simulation. In particular, we will focus our attention to examine whether the equilibrium of an FRC can be well-controlled by magnetic compression coils.

## 2. Numerical Model

As shown in Fig. 1, the confinement region in the FIX machine consists of the central confinement region and the mirror field region at its two ends. The central confinement region is 0.8m inner diameter and 3m long metal chamber. The confining magnetic field in this region is generated by solenoid coils. The strength of this magnetic field in vacuum  $B_0$  ranges from 0.01 to 0.08T. In our simulation, we fix  $B_0$  at 0.04T for typical experimental parameter. The both ends of confinement region are tapered to the 0.5m inner diameter. Therefore,

Corresponding author's e-mail: kanki@ppl.eng.osaka-u.ac.jp

the mirror field region on both ends is constructed. In this experiment, the strength of the upstream and downstream magnetic mirror field  $B_m$  are 0.13 and 0.17T, respectively. In the simulation, however, for simplicity we assume the confining magnetic flux in the central confinement region is conserved in the mirror field region on both ends. Hence, in accordance with  $B_0 = 0.04\text{T}$ , we set  $B_m = 0.1\text{T}$  as the strength of mirror field. The axial magnetic compression coils are coaxially installed in the confinement region as shown in Fig. 1. The three turn coils 0.66m diameter are equispaced by 0.2m. The strength of maximum compressing magnetic field  $B_c$  ranges from 0.05 to 0.15T and the typical rise time is about  $30\mu\text{sec}$ . The operation model in the simulation for this field is assumed that  $B_c$  rises sinusoidally between 0 and  $30\mu\text{sec}$ , thereafter kept constant value.

Let us use a cylindrical coordinate  $(z,r,\phi)$  in which the  $z$ -axis lies along the symmetry axis of the confinement chamber. We assume the axisymmetry, and carry out numerical simulations in a two dimensional  $(z,r)$  plane. As shown in Fig. 1, we divide the confinement region in which the simulation is performed into two regions. One is a vacuum subregion where the magnetic field is calculated only, and the other is a plasma subregion where the full set of magnetohydrodynamic (MHD) equations are solved. We use a perfect conducting boundary at the chamber wall. Further, free boundary conditions are imposed on the both open end boundaries of confinement region in order to reduce the reflection of MHD flow. Therefore, plasma is allowed to expand freely through the boundary. Since in general, an FRC has the sharp plasma pressure gradients in the vicinity of separatrix, it

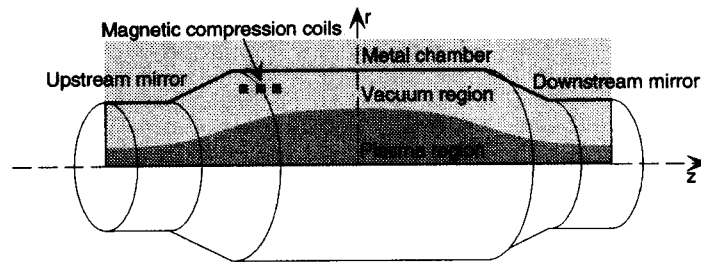


Fig. 1 Schematic view of the numerical system in cylindrical coordinate  $(z,r,\phi)$ . Shaded poloidal plane represents the two-dimensional simulation region.

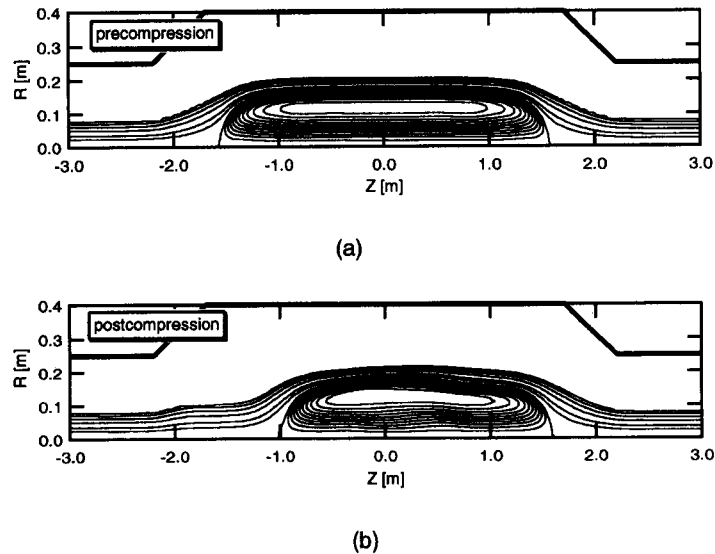


Fig. 2 Poloidal flux contours of FRC at applied compressing magnetic field of 0.05T: (a) precompression stage ( $0\mu\text{sec}$ ); (b) postcompression stage ( $40\mu\text{sec}$ ).

is required to concentrate the mesh on the region. As the computation mesh allowing the mesh to concentrate, we employ a Lagrangian mesh [5]. The interface between the vacuum and plasma moves with the plasma motion. Two temperature MHD model [6] that separate electron and ion temperature are calculated is used because the ion-electron collision time in the confinement region is much longer than the time scale of compression process. Resistive particle-field diffusion is calculated using classical resistivity. The effect of thermal conductivity follows Braginskii [7].

As the initial value for simulation, we use the numerically computed equilibrium with separatrix radius, (normalized by the wall radius at  $z = 0$ )  $x_s \approx 0.4$  such as typically observed in the FIX experiment. By applying a thermodynamic equation of state for an ideal gas, plasma density profile can be estimated from the assumption that the temperature is spatially uniform in the plasma region.

### 3. Numerical Results

We present the simulation results for the magnetic compression process of FRC plasmas. On the basis of these results, the effects of compressing magnetic field on FRC plasmas are investigated. Poloidal flux contours of FRC at applied compressing magnetic field of 0.05T are shown in Fig. 2, where only plasma region is plotted in the poloidal plane. Figure 2(a) shows the initial poloidal flux contours at precompression which are in equilibrium of FRC. In the postcompression, one can see that FRC plasma is axially compressed by compressing magnetic field. Namely, the magnetic compression process leads the initial long and thin FRC

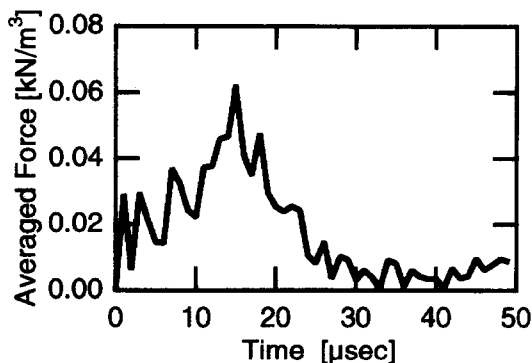


Fig. 3 Time evolution of spatially averaged force  $\langle |j \times B - \nabla p| \rangle$ , where  $j$ ,  $B$  and  $p$  denote the current density, magnetic field and plasma pressure, respectively.

( $r_s = 0.17\text{m}$ ,  $l_s = 3.15\text{m}$ ) to the final short and fat FRC ( $r_s = 0.19\text{m}$ ,  $l_s = 2.60\text{m}$ ). Here, more interestingly, the closed magnetic flux surfaces of FRC can be retained during the magnetic compression process.

In order to examine the motion of FRC plasma during magnetic compression process, we plot the temporal evolution of spatially averaged force  $\langle |j \times B - \nabla p| \rangle$  in Fig. 3. Between 0 and  $15\mu\text{sec}$  the FRC plasma is axially accelerated while repeating the dynamic radial bouncing motion. The existence of the bouncing motion means that the finite pressure gradient is not balanced with the Lorentz force because of the pressure increased by the enhanced Joule heating. After  $15\mu\text{sec}$  the averaged force begins to decrease to about zero. As a result, the MHD equilibrium condition of  $j \times B = \nabla p$  is approximately satisfied after compression ( $30\mu\text{sec}$ ).

Figures 4 and 5 show the radial profiles of the plasma pressure and the toroidal current density on the midplane. It is found from Fig.4 that the increased pressure profile due to the magnetic compression is broadened in the peaked part. In addition, the pressure gradients near the separatrix of postcompression are sharper than those of precompression. It is seen from Fig. 5 that the toroidal current density profile of postcompression is more hollow than that of precompression. The discontinuity of the current density profile outside the separatrix at precompression is due to the assumption of function form of pressure profile in the Grad-Shafranov equation.

Here, in order to evaluate the influence of the

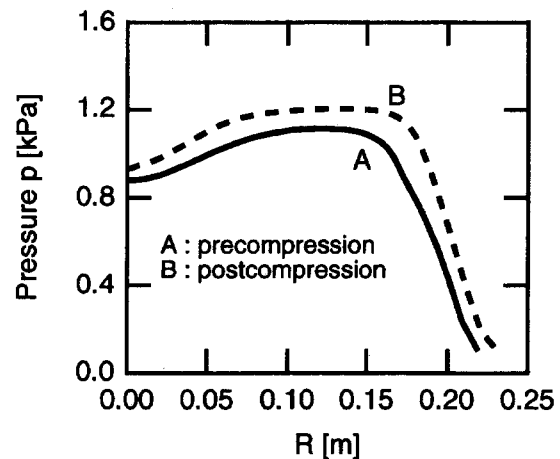


Fig. 4 Radial plasma pressure profiles at pre- and postcompression stages on the chamber midplane for same condition as Fig. 2.

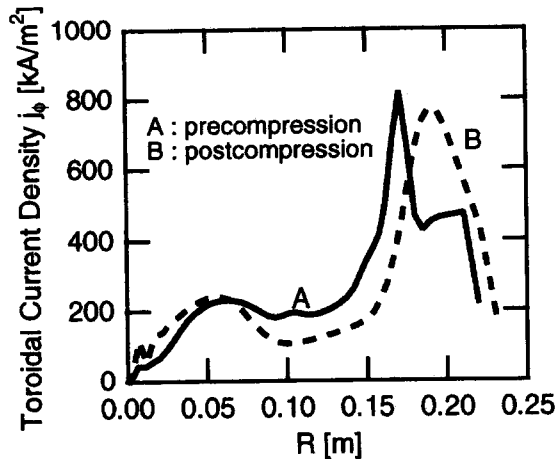


Fig. 5 Radial toroidal current density profiles at pre- and postcompression stages on the chamber midplane for same condition as Fig. 2.

compressing magnetic field on the equilibrium shape and radial current profile, several equilibrium characteristics are introduced. These are the separatrix elongation,  $E$ , the shape index,  $N$  (denoting the separatrix shape in the end region) and the current profile index,  $h$  (denoting the structure of the current profile) [8]. An  $N$  value nearly equal to  $E$  value reflects an elliptical separatrix, while an  $N$  value less than  $E$  value describes a racetrack separatrix. Furthermore, equilibria with  $h = 1$  are designated as having flat current profile;  $h < 1$  as hollow, and  $h > 1$  as peaked. These macroscopic quantities obtained from Figs. 2 and 5 are  $E = 9.2$ ,  $N = 6.0$  and  $h = 0.55$  for precompression, and  $E = 7.0$ ,  $N = 7.1$  and  $h = 0.35$  for postcompression. Here,  $N$  values are estimated from the separatrix shape of the upstream side. The separatrix shape for this case changes from racetrack type to elliptical one, whereas

current profile becomes more hollow. The increase in  $N$  value is ascribed to the strength of the compressing magnetic field weaker than that of initial mirror field. From the above simulation results, the equilibrium shape and radial profile (i.e., pressure and current) can be well-controlled by applying external compressing field.

#### 4. Conclusions

We have investigated the effects of compressing magnetic field on FRC plasmas by using the MHD simulation. It is concluded from the simulation results that the equilibrium shape and profiles of pressure and current can be well-controlled by axial magnetic compression. Concerning the equilibrium control, these results have analogies to the effects of external mirror field on FRCs. However, it is predicted that the effects of axial magnetic compression are more available in the wide variety of equilibrium shape and radial profiles than those of the mirror field.

#### References

- [1] S. Okada *et al.*, *Proc. ICPP*, 1182 (1996).
- [2] K.F. McKenna *et al.*, *Phys. Rev. Lett.* **50**, 1787 (1983).
- [3] H. Himura *et al.*, *Phys. Plasmas* **2**, 191 (1995).
- [4] S. Okada *et al.*, *Proc. 17th IAEA Fusion Energy Conf.*, Yokohama, Japan, 19–24 Oct., (1998), to be published in IAEA-CN-69/EXP4/14.
- [5] J.U. Brackbill and W.E. Pracht, *J. Comp. Phys.* **13**, 455 (1973).
- [6] N. Mizuguchi, *private communication*.
- [7] S.I. Braginskii, *Reviews of Plasma Physics*, ed. M.A. Leontovich (Consultants Bureau, New York, 1965), Vol. 1, p. 205.
- [8] L.C. Steinhauer *et al.*, *Phys. Plasmas* **1**, 1523 (1994).